Received 7 June 2021; revised 20 July 2021; accepted 20 July 2021. Date of publication 26 July 2021; date of current version 13 December 2021.
The review of this article was arranged by Editor S. Ikeda

Digital Object Identifier 10.1109/JEDS.2021.3099494

Dynamic Ron Effect in GaN HEMT in a Zero-Voltage-Switching Circuit Due to Off-Resonance Operation

SHAOYU SUN [1,2], LING XIA [3], WENGANG WU [2], AND YUFENG JIN [1,2]

1 Shenzhen Graduate School, Peking University, Shenzhen 518055, Guangdong, China
2 Institute of Microelectronics, Peking University, Beijing 100871, China
3 Research and Development, Shenzhen Hai Li Technology Inc., Shenzhen 518100, China

CORRESPONDING AUTHOR: Y. JIN (e-mail: yfjin@pku.edu.cn)

This work was supported in part by the TSV 3D Integrate Micro/Nanosystem Lab under Grant ZDSYS201802061805105, and in part by the Natural Science Foundation of Shenzhen under Grant JCYJ20190808155007550.

ABSTRACT Dynamic ON resistance of GaN devices is a must-care point for users. In this paper, the reverse conduction of commercial GaN power transistors is studied. Even though the commercial HEMTs show stable performance in normal operation modes (off-to-on), significant dynamic ON resistance can be seen in some particular conditions. A test method is set up to evaluate dynamic R_{on} in a reverse-to-on mode. The conditions to activate the behavior are discussed, and the cause of dynamic R_{on} is possibly due to traps located in the gate region. Meanwhile, a wireless power transfer system operating at 6.78MHz is used to study the effect of reverse conduction mode on dynamic resistance at the circuit level. According to the change of the operation frequency, we find that the influence of reverse conduction on the dynamic R_{on} effect is not only affected by the value of reverse conduction voltage but also related to the operating mode of the device.

INDEX TERMS GaN, dynamic resistance, wireless power transfer, reverse conduction.

I. INTRODUCTION

GaN HEMT is emerging as a promising candidate for next-generation power switching applications [1]. Throughout the years, many kinds of application schemes for GaN HEMT had been proposed. But one critical factor that needs solving before such a new scheme can address a mass market is its reliability [2], [3].

One of the reasons that cause reliability problems in GaN devices is the dynamic ON-resistance (R_{on}) effect [4]. Dynamic R_{on} characteristics, the fact that GaN HEMT R_{on} does not remain constant, has attracted much attention. It will seriously limit the output power and efficiency of the device [5]. In addition, dynamic R_{on} could also cause reliability problems when the device operates for a long time [6].

However, most of the previous studies focus on off-state stress and the on-state behavior of GaN HEMT [7]. What happens in reverse conduction for GaN needs much more understanding. Despite the disproportionally little attention it has drawn, reverse conduction is quite common in systems with an inductive or an LC resonant load.

In recent years, magnetic resonance wireless power transfer (WPT) has developed rapidly because of its advantages, such as long transmission distance and high efficiency [8]. AirFuel standard (A4WP) stipulates that the operation frequency of magnetic resonance wireless power transfer is 6.78MHz [9]. Compared with Si power devices, GaN HEMT is more suitable for this application.

In this paper, we studied the influence of reverse conduction on the dynamic R_{on} effect of commercial GaN devices. Firstly, we built a special test circuit that makes the device operate in a reverse-to-on mode to study the dynamic R_{on} effect on the device level. Secondly, a class-D zero-voltage-switching (ZVS) magnetic resonance WPT system with an LC resonant tank is built using GaN HEMT to observe the influence of reverse conduction mode on the dynamic R_{on} of the device on the circuit level. LTspice is used for simulation analysis. The original study is done in a WPT system. But

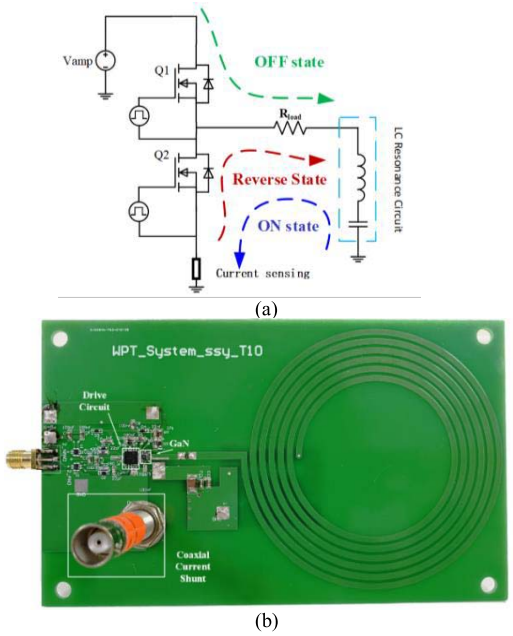

FIGURE 1. **(a) Simplified circuit diagram of the GaN half-bridge WPT system studied. (b) Photo of the transmitter of the magnetic resonance WPT system.**

the findings can be general for other systems with a similar mode of operations.

II. EXPERIMENT AND METHOD

Fig. 1(a) shows a schematic of the WPT system. Reference [10] explains the details of this circuit. R_{load} is the equivalent resistance mapped to the transmission side from the receiver load. Three current paths are corresponding to the three states in Fig. 1(a). When Q_2 turns off, and Q_1 turns on, the current charges the LC resonance tank along the green line. Before Q_2 turns on and Q_1 turns off, there is a dead time when both GaN HEMTs are off. At the same time, the inductor current must be continuous, which makes Q_2 operate in the reverse state (red line). After that, Q_2 turns on, while Q_1 turns off. The current flows along the blue line. Compared with the off-to-on mode in most previous studies, a special operation mode exists for Q_2: off-reverse-on.

Fig. 1(b) shows the photo of the magnetic resonance WPT system. Two EPC2107 GaN HEMTs were used to form a half-bridge [11]. The chip (EPC2017) consists of three transistors, two of which serve as half-bridge circuits and one that replaces the diode in the bootstrap circuit. R_{on} of the low-side GaN HEMT (Q_2) was measured, and the DC characteristics are shown in Fig. 2. The drive circuit chip used LM5113 produced by Texas Instruments. A coaxial current shunt (part SSDN-10 manufactured by T&M Research Products Inc.) is used to detect the current flowing through the Q_2 [12]. The reverse conduction can be further observed from the voltage waveform of Q_2, as shown in Fig. 3. The negative overshoot indicates the reverse state of Q_2.

To evaluate the effect of the reverse state on R_{on}, a special operation mode, reverse-to-on, is constructed through a separate setup shown in Fig. 4. V_{amp} and V_R are DC power

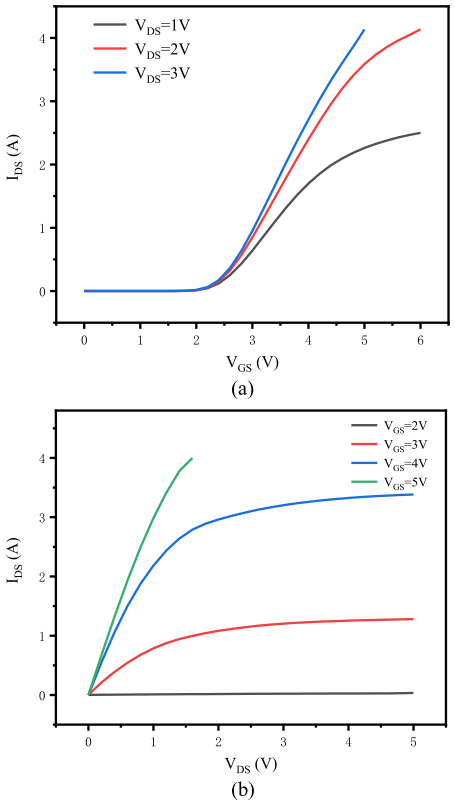

FIGURE 2. **DC performance of the Q_2 (EPC2107) which is tested by Keysight B1505A. (a) The transfer characteristic of the Q_2 under different V_{DS}. (b) The output characteristic of Q_2 under different V_{GS}.**

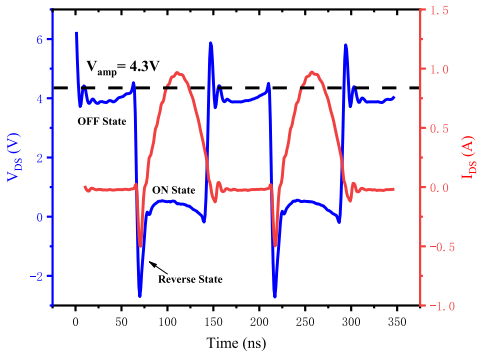

FIGURE 3. **Measured V_{DS} and I_{DS} for Q_2 in a real WPT system. The V_{amp} is 4.3 V, and the test frequency is 6.78MHz. The $V_{GS\text{-}On\ State}$ is 5 V.**

sources. Q_1 and Q_2 are turned on and off at the same time. For Q_2, V_{amp} provides a positive voltage at on state. V_R provides a negative voltage and introduces reverse conduction. In Fig. 4 (a), the current flows through Q_2 when both devices are turned on. When the devices are off (V_{GS} is 0 V), Q_2 operates in a reverse state (Fig. 4 (b)).

The R_{on} of the low-side GaN device (Q_2) is measured in on state. The setup senses the voltage (V_{DS}) and current (I_{DS}) of Q_2 in real-time. V_{DS} can be obtained using an oscilloscope. A coaxial current shunt is used to detect the current. One example of the V_{DS} and I_{DS} waveforms is shown in Fig. 5. With caution, we can accurately measure

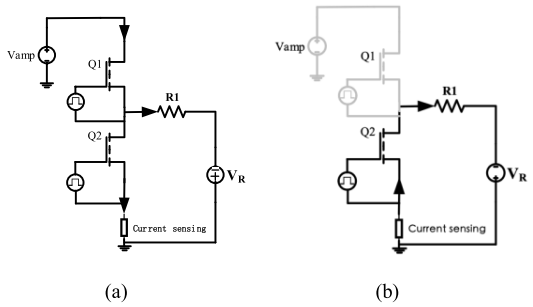

FIGURE 4. A special test circuit to make the Q_2 operate in reverse-to-on mode. (a) The Q_2 operates in an on state. (b) The Q_2 operates in a reverse state.

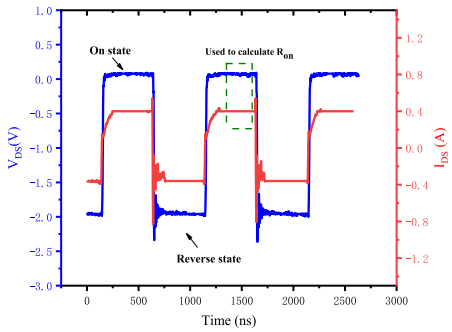

FIGURE 5. The V_{DS} (blue) and I_{DS} (red) are the waveforms of Q_2 operating in reverse-to-on mode. The V_{amp} is 0.3 V, and the test frequency is 1 MHz.

$R_{on} = V_{DS}/I_{DS}$ by averaging the data in the dotted box in Fig. 5.

The ON-state current is kept at 0.4 A to avoid R_{on}'s change due to the bias condition (I_{DS}) shift. A limited number of pulses are transmitted to the gate to reduce the impact of self-heat effect.

III. RESULT AND DISCUSSION

A. EFFECT OF REVERSE CONDUCTION IN DEVICE LEVEL

Fig. 6 shows the R_{on} with $V_{SD\text{-}Reverse\ State}$ under different $V_{GS\text{-}On\ State}$ (the test circuit is shown in Fig. 4). R_{on} increases the most when $V_{SD\text{-}Reverse\ State}$ is high and $V_{GS\text{-}On\ State}$ is low. According to the official EPC report: When the R_{on} of the device under dynamic conditions exceeds the static value by 20 %, it is considered that the device has a dynamic R_{on} [13]. For $V_{GS\text{-}On\ State}$ of 4 V, with the $V_{SD\text{-}Reverse\ State}$ increases from 0 V to 2V. R_{on} increases from 0.33 Ω to 0.55 Ω, or over 60 % (green curve). It is illustrated that the device has a dynamic R_{on} effect in this mode. This rise in the dynamic R_{on} is dangerous for the circuit, which brings risks to the system.

The device turns on at reverse state, relying on V_{SD} (V_{GS} is 0 V). The V_{SD}– I_{SD} is shown in the inset of Fig. 6. With the increase of $V_{SD\text{-}Reverse\ State}$ in this mode, the generation of dynamic R_{on} of the device requires the device to turn on at reverse state.

To determine whether such behavior (Fig. 6) is due to reversely biasing the gate [14], we performed the test in

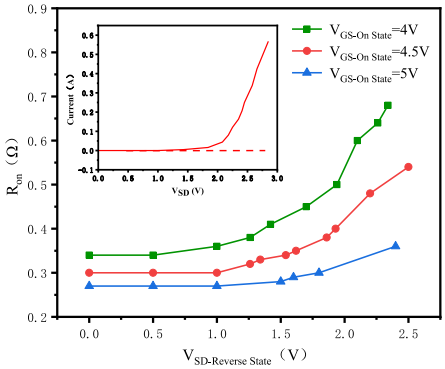

FIGURE 6. R_{on} changes with $V_{SD\text{-}Reverse\ State}$ under different $V_{GS\text{-}On\ State}$. The circuit operation frequency is 1 MHz, and V_{amp} is less than 1 V to guarantees the $I_{DS\text{-}On\ State}$ = 0.4A. The insert figure is the V_{SD} – I_{SD} of the device under V_{GS} is 0 V. As the V_{SD} exceeds 1.25 V, the device will produce the reverse current.

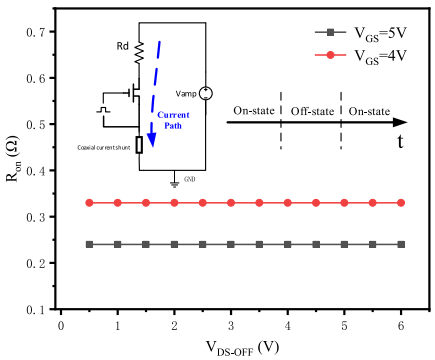

FIGURE 7. The device operates in a traditional switching mode (1 MHz). The red curve is with V_{GS} of 4 V. The black curve is with V_{GS} of 5 V. The test circuit is in the upper left corner.

Fig. 7. The device operates in a traditional on-to-off switching mode. In such a case, the gate-to-drain diode is reversely biased in an off state. As the $V_{DS\text{-}OFF}$ reaches 6 V, there is little dynamic R_{on} in both curves. Hence, the answer to the question is negative.

We have swapped the source and drain's position of the device Q_2 in Fig. 4 and repeated the measurement. The source of the Q_2 is connected to Q_1, and the drain is connected to current sensing. A similar dynamic R_{on} phenomenon shows up in this condition. Therefore, such behavior is not because the drain is further away from the gate than the source.

This dynamic R_{on} effect also depends on the operating frequency. Fig. 8 shows that as the frequency increases above 300 kHz, the red curve rises rapidly, while the black curve remains almost unchanged. Therefore, the higher the operating frequency, the greater the influence of reverse conduction on the dynamic R_{on} [15].

Given the experimental data above, we postulate that certain types of shallow traps exist underneath the gate. They might be from the gate, the AlGaN barrier [16], or the GaN buffer [17]. The most likely location of the traps is in the gate, though the exact position is still under investigation.

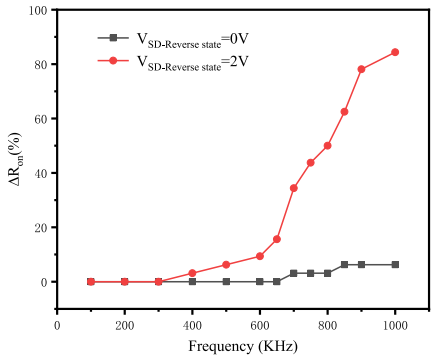

FIGURE 8. Dynamic R_{on} is a function of frequency. V_{GS} is 4 V. The black curve is $V_{SD\text{-}Reverse\ State}$ = 0 V, and the red curve is $V_{SD\text{-}Reverse\ State}$ = 2 V. The frequency increases from 100 kHz to 1 MHz. The V_{amp} is 0.4 V.

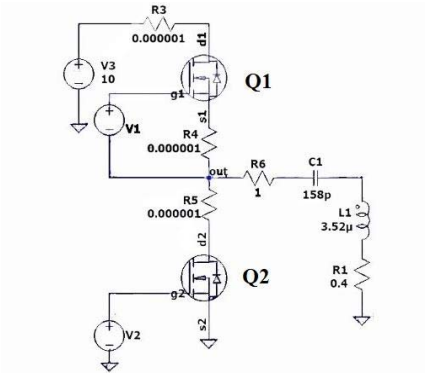

FIGURE 9. The schematic of magnetic resonance WPT system simulated by LTspice.

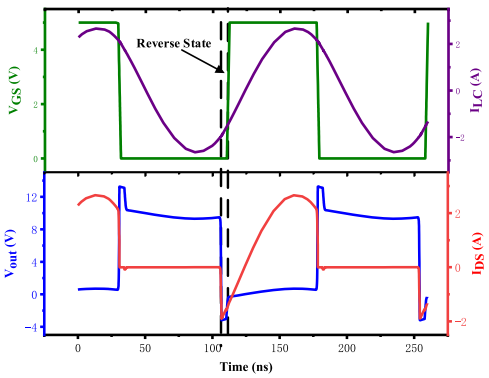

FIGURE 10. The reverse state appears for the device (Q_2) in a WPT system. The V_{amp} is 10V. The green, red and blue curves are V_{GS}, I_{DS}, and V_{DS}, respectively, for Q_2 (in Fig. 9). The purple curve is the current flowing through the LC tank.

Several factors are needed to activate these traps: 1) some mild positive bias across the gate, so the device is not fully turned on (semi-on state). 2) Enough reverse conduction voltage ($V_{SD\text{-}Reverse\ State}$). 3) Significant channel current to provide the source of electrons. 4) A proper operating frequency, probably determined by the time constants of these traps. As the phenomenon becomes more obvious with higher frequency, these are likely shallow traps [18].

One mechanism can explain this phenomenon. When the device is reverse conducting, the value of $V_{SD\text{-}Reverse\ State}$ is much higher than the normally $V_{DS\text{-}On\ state}$. The higher $V_{SD\text{-}Reverse\ State}$ will generate a larger electric field in the device channel, and the $I_{SD\text{-}Reverse\ State}$ provides a source of electrons. It will make the hot electron effect more likely to occur and lead R_{on} of the device to increase under high operation frequency [19], [20].

B. EFFECT OF REVERSE CONDUCTION IN CIRCUIT LEVEL

One factor that causes the device to appear reverse conduction in the system is the operating frequency. In a real WPT system, because the uniformity and processing accuracy of the components may cause the resonant frequency of the LC tank ($f_{LC\ tank}$) to deviate from the operating frequency ($f_{operation}$). So in this part, we study the influence of reverse conduction on the dynamic R_{on} of the device under different operating frequency.

First, we explain the reason why reverse conduction appears when the $f_{LC\ tank}$ deviates from the $f_{operation}$. Fig. 9 is the schematic of the LTspice simulation circuit for the WPT system. V_1 and V_2 can generate square wave signals ($V_{GS\text{-}On\ State}$ = 5 V) with a phase difference of 180°. The model of the GaN device (GaN EPC2107) is from the EPC official website. The V_{amp} is a DC power source. C_1 and L_1 are composed of LC resonance circuit (LC tank). R_6 is Equivalent load resistance and R_1 is parasitic resistance coming from layout, packaging, and so on.

Fig. 10 is our simulation result. The $f_{operation}$ is 6.8 MHz which is higher than $f_{LC\ tank}$ (6.78MHz). Because $f_{operation} > f_{LC\ tank}$, the inductive of the LC tank causes the phase displacement between input current (I_{LC}) and voltage (V_{out}) [21]. To ensure the continuity of the inductor current, the reverse conduction appears for the device when V_{GS} = 0 V (between two dashed lines). The reverse conduction voltage ($V_{SD\text{-}Reverse\ State}$) is related to I_{LC} and $f_{operation}$.

Fig. 11 shows the operation mode of the GaN device under different $f_{operation}$ in the WPT system. When $f_{operation} < f_{LC\ tank}$, the GaN device operation in off-on-reverse mode (Fig. 12 (a)) within one cycle. When $f_{operation} = f_{LC\ tank}$, the device reaches the ideal operating state and operates in off-to-on mode (Fig. 13 (b)). When $f_{operation} > f_{LC\ tank}$, the GaN device operates in off-reverse-on mode (Fig. 11 (c)).

Fig. 12 shows the relationship between the ΔR_{on} of the device and reverse-conducting time under different $V_{SD\ Reverse\ State}$. When the $V_{SD\ Reverse\ State}$ exceeds 1.5 V, the device will reverse conduction. So there is no dynamic R_{on} effect on the blue curve. The device has a dynamic R_{on} effect when the reverse conduction time exceeds 14 ns for the red curve. As the reverse conduction time increases, the dynamic R_{on} effect continues to deteriorate (ΔR_{on} = 54% at $T_{Reverse\ State}$ is 32 ns). It is illustrated that the deterioration of the dynamic R_{on} of the device is both related to the $V_{SD\ Reverse\ State}$ and the reverse conduction time.

Fig. 13 shows the measurement result of the R_{on} and I_{LC} at different $f_{operation}$ in a real WPT system. Fig. 1 (b) is

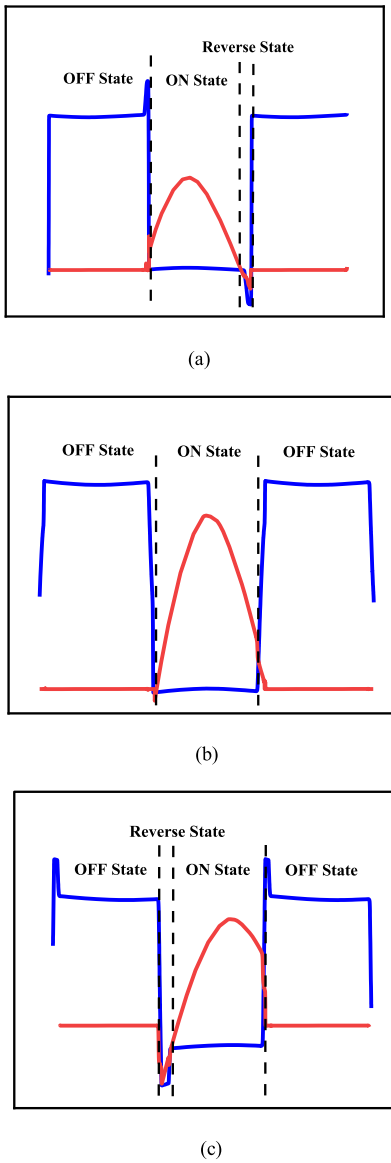

FIGURE 11. The operation mode of the device (Q_2) under different operation frequencies in one cycle. The blue curve is the V_{DS}, and the red curve is the I_{DS} of the Q_2.

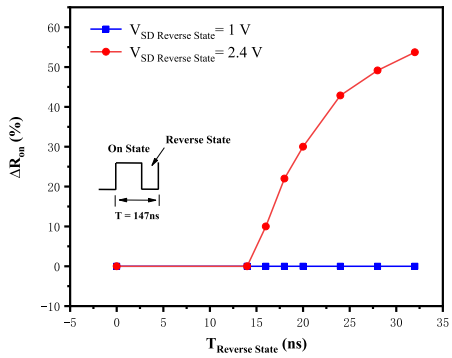

FIGURE 12. The relationship between ΔR_{on} and reverse state time. The test circuit is shown in Fig. 3. The test frequency is 6.78MHz, and the $V_{GS\text{-}on\ State}$ is 5 V. The blue curve is $V_{SD\ Reverse\ State}$ = 1 V, and the red curve is $V_{SD\ Reverse\ State}$ = 2.4 V.

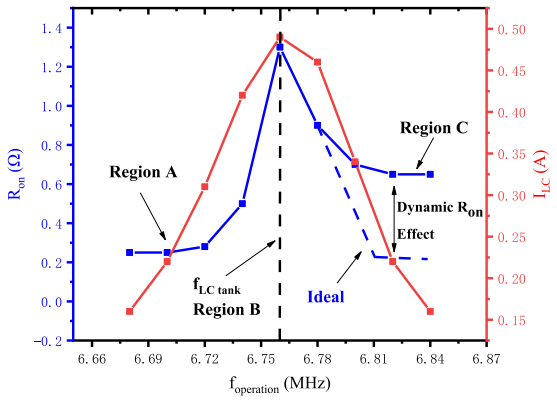

FIGURE 13. The blue curve is the R_{on} of the GaN device (Q_2) and the red curve is I_{LC} (RMS) for the WTP system. The X-axis is $f_{operation}$.

the photo of the WPT system, and Fig. 9 is the schematic of this system. In Fig. 13, the region A, region B, and region C corresponds to the Q_2 operating in Fig. 11 (a), Fig. 11 (b), and Fig. 11 (c) modes, respectively. In our test, the $V_{GS\text{-}On\ State}$ is 5 V (recommended by vendor) and the V_{amp} = 5 V. The $f_{LC\ tank}$ is 6.76 MHz, and load resistance (R_6 in Fig. 9) is 0 Ω. In Fig. 13, the red curve reaches its maximum value (0.48 A) when $f_{operation} = f_{LC\ tank}$ at 6.76 MHz (black dotted line) and decreases as the $f_{operation}$, and $f_{LC\ tank}$ deviation are greater. The changing trend of the R_{on} is similar to the I_{LC}. The difference is that the R_{on} in region A is 0.25 Ω, while it is 0.6 Ω in region C.

The variation of the red curve can be explained by equation (1). When $f_{operation} = f_{LC\ tank}$, $Z_{LC\ tank}$ is the smallest and the I_{LC} of the system is the largest. When $f_{operation}$ deviates from the $f_{LC\ tank}$, the $Z_{LC\ tank}$ increases and the I_{LC} decreases.

$$Z_{LC\ tank} = 2\pi L f_{operation} + \frac{1}{2\pi C f_{operation}}. \tag{1}$$

For the blue curve, in the region I, I_{LC} is small and the R_{on} is the same as the static value of the device. As the $f_{operation}$ rises, the larger I_{LC} makes the self-heating effect more serious, leading to the R_{on} of the device increasing [22]. Ideally. in region C, the small I_{LC} makes R_{on} decrease, such as the blue dotted line. However, in region C (solid line), the R_{on} of the device (0.6 Ω) is increased by 140 % compared to the region A (0.25 Ω) in our test. A noticeable dynamic R_{on} effect appears in this operating condition.

The simulation (LTspice) is used to analyze this phenomenon in Fig. 14. The vary of the I_{LC} is the same as the test results in Fig. 13. The blue curve is the reverse conduction voltage ($V_{SD\text{-}Reverse\ State}$). Three regions are shown in Fig. 14, which is the same as Fig. 13. When the system is operating in region A and region C, reverse conduction is both appeared. In our test (Fig. 13), the $V_{SD\text{-}Reverse\ State}$ can reach 4 V in region A and region C, which is similar to the simulation results. But in Fig. 13, only the dynamic R_{on} effect appears in region C. It is illustrated that the influence of reverse conduction on the dynamic R_{on} effect is also related to the operating mode of the device.

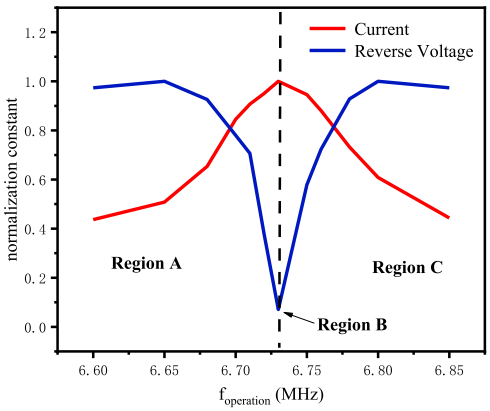

FIGURE 14. The simulation of the device in different operating frequencies. The schematic of the circuit is shown in Fig. 9. The red curve is I_{LC}, and the blue curve is reverse voltage ($V_{SD\text{-}Reverse\ State}$).

We consider that the cause of this phenomenon is likely to be related to the traps inside the device, but the specific trap characteristics and mechanisms are still under study.

IV. CONCLUSION

In this research, we study the influence of reverse conduction on the dynamic characteristics of commercial GaN devices. A special reverse-to-on mode is used to study the device's dynamic R_{on} effect at the device level. The dynamic R_{on} is highly probable to appear in high $V_{SD\text{-}Reverse\ State}$, low $V_{GS\text{-}On\ state}$ and high frequency. The cause of dynamic R_{on} may be the traps located in the gate region. The traps might be induced by non-uniform material growth or device processing. Because more than 50 devices are tested in the experiment. These devices come from different batches. About 60% of these devices show dynamic R_{on} in this mode of operation. Our research considers that for EPC2107, the reverse conduction voltage should be less than 2V (when $V_{GS\text{-}On\ State} = 5$ V).

At the circuit level, we analyze the device operation mode under different operating frequency. We found that the dynamic R_{on} effect of the device is not only affected by the value of reverse conduction voltage but also related to the operating mode of the device in the system. Compared with the off-on-reverse mode, the off-reverse-on mode could make the dynamic R_{on} more susceptible to reverse conduction. Meanwhile, we suggest that future reliability standards consider including the test measurement mentioned in this paper to ensure the reliability of product operation.

REFERENCES

[1] H.-S. Chen *et al.*, "Combining high hole concentration in p-GaN and high mobility in u-GaN for high p-Type conductivity in a p-GaN/u-GaN alternating-layer nanostructure," *IEEE Trans. Electron Devices*, vol. 64, no. 1, pp. 115–120, Jan. 2017, doi: 10.1109/TED.2016.2631148.

[2] D. Jin and J. A. del Alamo, "Mechanisms responsible for dynamic ON-resistance in GaN high-voltage HEMTs," in *Proc. 24th Int. Symp. Power Semicond. Devices ICs*, 2012, pp. 333–336, doi: 10.1109/ISPSD.2012.6229089.

[3] G. Meneghesso, M. Meneghini, and E. Zanoni, "Reliability and instabilities in GaN-based HEMTs," in *Proc. IEEE Int. Conf. Electron Devices Solid-State Circuits*, 2014, pp. 1–2, doi: 10.1109/EDSSC.2014.7061275.

[4] A. Chini and F. Iucolano, "Experimental and numerical evaluation of RON degradation in GaN HEMTs during pulse-mode operation," *IEEE J. Electron Devices Soc.*, vol. 5, no. 6, pp. 491–495, Nov. 2017, doi: 10.1109/JEDS.2017.2754859.

[5] P. Moens *et al.*, "On the impact of carbon-doping on the dynamic Ron and off-state leakage current of 650V GaN power devices," in *Proc. IEEE 27th Int. Symp. Power Semicond. Devices ICs (ISPSD)*, Hong Kong, 2015, pp. 37–40, doi: 10.1109/ISPSD.2015.7123383.

[6] E. Zanoni, M. Meneghini, G. Meneghesso, D. Bisi, I. Rossetto, and A. Stocco, "Reliability and failure physics of GaN HEMT, MIS-HEMT and p-gate HEMTs for power switching applications: Parasitic effects and degradation due to deep level effects and time-dependent breakdown phenomena," in *Proc. IEEE 3rd Workshop Wide Bandgap Power Devices Appl. (WiPDA)*, 2015, pp. 75–80, doi: 10.1109/WiPDA.2015.7369305.

[7] S. Sun, J. Zhang, L. Xia, W. Wu, J. Wang, and Y. Jin, "Impact of E-mode gallium nitride high electron mobility transistor with P-type gate on waveform distortion in an AirFuel wireless power transfer system," *Physica Status Solidi (A)*, vol. 218, no. 3, 2021, Art. no. 2000565, doi: 10.1002/pssa.202000565.

[8] Y. Wang, J. Song, L. Lin, X. Wu, and W. Zhang, "Research on magnetic coupling resonance wireless power transfer system with variable coil structure," in *Proc. IEEE PELS Workshop Emerg. Technol. Wireless Power Transf. (WoW)*, Chongqing, China, 2017, pp. 1–6, doi: 10.1109/WoW.2017.7959403.

[9] S. Sun, L. Xia, W. Wu, and Y. Jin, "Reverse conduction induced dynamic R_{on} effect in GaN HEMT with p-GaN gate," in *Proc. 5th IEEE Electron Devices Technol. Manuf. Conf. (EDTM)*, Chengdu, China, 2021, pp. 1–3, doi: 10.1109/EDTM50988.2021.9420891.

[10] S. Sun, J. Zhang, W. Wu, L. Xia, and Y. Jin, "Mechanism of wireless power transfer system waveform distortion caused by nonideal gallium nitride transistor characteristics," *Chin. J. Elect. Eng.*, vol. 7, no. 2, pp. 61–69, Jun. 2021, doi: 10.23919/CJEE.2021.000016.

[11] *EPC2107—Enhancement Mode GaN Power Transistor Half Bridge With Integrated Synchronous Bootstrap*. Accessed: Jun. 25, 2021. [Online]. Available: https://epc-co.com/epc/Products/eGaNFETsandICs/EPC2107.aspx

[12] Z. Liu, X. Huang, F. C. Lee, and Q. Li, "Package parasitic inductance extraction and simulation model development for the high-voltage cascode GaN HEMT," *IEEE Trans. Power Electron.*, vol. 29, no. 4, pp. 1977–1985, Apr. 2014, doi: 10.1109/TPEL.2013.2264941.

[13] *EPC*. Accessed: Jun. 25, 2021. [Online]. Available: https://epc-co.com/epc/Portals/0/epc/documents/product-training/EPC_relreport_030510_finalfinal.pdf

[14] Q. Zhu *et al.*, "Investigation of inverse piezoelectric effect and trap effect in AlGaN/GaN HEMTs under reverse-bias step stress at cryogenic temperature," *IEEE Access*, vol. 8, pp. 35520–35528, 2020, doi: 10.1109/ACCESS.2020.2975118.

[15] S. Yang *et al.*, "Investigation of SiNx and AlN passivation for AlGaN/GaN high-electron-mobility transistors: Role of interface traps and polarization charges," *IEEE J. Electron Devices Soc.*, vol. 8, pp. 358–364, Mar. 2020, doi: 10.1109/JEDS.2020.2984016.

[16] S. Huang, Q. Jiang, S. Yang, Z. Tang, and K. J. Chen, "Mechanism of PEALD-grown AlN passivation for AlGaN/GaN HEMTs: Compensation of interface traps by polarization charges," *IEEE Electron Device Lett.*, vol. 34, no. 2, pp. 193–195, Feb. 2013, doi: 10.1109/LED.2012.2229106.

[17] J.-H. Lee *et al.*, "High figure-of-merit (V_{BR}^2/R_{ON}) AlGaN/GaN power HEMT with periodically C-doped GaN buffer and AlGaN back barrier," *IEEE J. Electron Devices Soc.*, vol. 6, pp. 1179–1186, Oct. 2018, doi: 10.1109/JEDS.2018.2872975.

[18] T. A. G. Eberlein *et al.*, "Shallow acceptors in GaN," *Appl. Phys. Lett.*, vol. 91, no. 13, 2007, Art. no. 132105, doi: 10.1063/1.2776852.

[19] G Meneghesso *et al.*, "Reliability and parasitic issues in GaN-based power HEMTs: A review," *Semicond. Sci. Technol.*, vol. 31, no. 9, 2016, Art. no. 093004, doi: 10.1088/0268-1242/31/9/093004.

[20] A. Minetto *et al.*, "Hot-electron effects in AlGaN/GaN HEMTs under semi-ON DC stress," *IEEE Trans. Electron Devices*, vol. 67, no. 11, pp. 4602–4605, Nov. 2020, doi: 10.1109/TED.2020.3025983.

[21] A. Teramoto, R. Kuroda, M. Komura, K. Watanabe, S. Sugawa, and T. Ohmi, "Capacitance-voltage measurement method for ultrathin gate dielectrics using LC resonance circuit," *IEEE Trans. Semicond. Manuf.*, vol. 19, no. 1, pp. 43–49, Feb. 2006, doi: 10.1109/TSM.2005.863230.

[22] Y. Zhang, S. Feng, H. Zhu, C. Guo, B. Deng, and G. Zhang, "Effect of self-heating on the drain current transient response in AlGaN/GaN HEMTs," *IEEE Electron Device Lett.*, vol. 35, no. 3, pp. 345–347, Mar. 2014, doi: 10.1109/LED.2014.2300856.